
Title	A methodology to design and fabricate a smart brace using low-cost additive manufacturing
Author(s)	P. S. P. Teng, K. F. Leong, P. W. Kong, B. H. Er, Z. Y. Chew, P. S. Tan and C. H. Tee

Copyright © 2022 Taylor & Francis

This is an Accepted Manuscript of an article published by Taylor & Francis in *Virtual and Physical Prototyping*, on 29/06/2022, available online:
<https://doi.org/10.1080/17452759.2022.2090384>

1 **A Methodology to Design and Fabricate a Smart Brace using Low-Cost Additive**

2 **Manufacturing**

3

4 **P.S.P. Teng ^{a,b#}, K.F. Leong ^{*a,b}, P.W. Kong ^c, B.H. Er ^b, Z.Y. Chew^b, P.S. Tan^b, C.H.**

5 **Tee^b**

6 ^a Singapore Centre for 3D Printing, Nanyang Technological University, 50 Nanyang Avenue,

7 Singapore 639798, Singapore

8 ^b School of Mechanical and Aerospace Engineering, Nanyang Technological University, 50

9 Nanyang Avenue, Singapore 639798, Singapore

10 ^c Physical Education and Sports Science Academic Group, National Institute of Education,

11 Nanyang Technological University, 1 Nanyang Walk, Singapore 637616, Singapore

12

13 [#] Rehabilitation Research Institute of Singapore, Nanyang Technological University, 50

14 Nanyang Avenue, Singapore 639798, Singapore (new affiliation after research was

15 conducted)

16 **Contact information for corresponding author:**

17 * LEONG Kah Fai (Corresponding author)

18 Nanyang Technological University

19 50 Nanyang Avenue, Singapore 639798

20 Tel: (65) 6790 5503

21 Email: mkfleong@ntu.edu.sg

22

23 This is an Accepted Manuscript of an article published by Taylor & Francis in Virtual and

24 Physical Prototyping, available online: <https://doi.org/10.1080/17452759.2022.2090384>.

25

26
27
28
29
30
31
32
33
34
35
36
37
38
39
40
41
42
43
44
45
46
47
48
49
50

A Methodology to Design and Fabricate a Smart Ankle Brace using Low-Cost Additive Manufacturing[†]

Abstract

Ankle braces typically restrict the functional range of motion. Braces should preferably allow a free functional range of motion during sport, while protecting the foot at high-risk positions beyond that range. This could be achieved with 3D printed metamaterial structures that could have varying properties throughout an individual’s ankle range of motion. This paper aims to illustrate an exploratory methodology of using an affordable Fused Deposition Modelling 3D printing technology to develop an ankle brace using metamaterial structures. It also showcases the design, manufacturing processes and testing of 3D printed customized ankle brace prototype designs that incorporated metamaterial structures. Initial tests showed that as designed, the prototype braces maintained the full range of motion for plantar flexion angles. Results also showed that the prototypes required one of the lowest moments during functional range of motion, while achieving almost twice to thrice the moment required beyond the functional range of motion.

Word Count: 150 words

Keywords: Ankle sprain, Metamaterial structures, Biomimetic, Anisotropic material properties, Tensile testing.

51 †A Patent Application (US Patent Application no.: 17/052,506) incorporating parts of this paper has been filed.

52 **1. Introduction**

53 An ankle sprain is common during sport and can lead to persistent pain, ankle instability and
54 possibly re-injury (Chen, McInnis, and Borg-Stein 2019). Ankle braces are being used to
55 prevent ankle injuries (Bot and van Mechelen 1999; Cordova, Ingersoll, and LeBlanc 2000;
56 Kaminski, Needle, and Delahunt 2019; Parsley et al. 2013). However, in doing so, ankle braces
57 could also limit the range of motion, such as those of the ankle plantar flexion angles (Mann,
58 Gruber, Murphy, and Docherty 2019). Limiting the functional range of motion could, in turn,
59 reduce force absorption and increase vertical ground reaction force, leading to other injuries
60 such as a bone fracture (Alentorn-Geli et al. 2009; Rowley and Richards 2015). Braces that
61 could allow a free functional range of motion during sport, while protecting the foot at high-
62 risk positions could bring about a revolutionary change to ankle brace designs. This could be
63 achieved with materials with varying properties throughout an individual's ankle range of
64 motion.

65 Metamaterials have become increasingly popular, especially with the progress of
66 additive manufacturing or three-dimensional (3D) printing (Zadpoor 2016). Metamaterials,
67 normally formed by repeated structures, have properties obtained from their structure rather
68 than the material itself (Paulose, Meeussen, and Vitelli 2015). These 3D printed metamaterials
69 thus present opportunities for personalised ankle braces to have varying properties through the
70 joint range of motion, as opposed to fixed properties and structures in most commercial ankle
71 braces. Materials are also often limited to proprietary materials that come with 3D printers, and
72 metamaterials could be designed to achieve unique properties that are required for the design
73 purpose and individual needs.

74 Personalised 3D printed orthoses are also relatively easy to manufacture compared to
75 traditional methods (Cha et al. 2017; Santos et al. 2017). Conventional customized methods
76 may require casts to be pre-manufactured or milled from a solid block resulting in design

77 constraints (Telfer et al. 2012), tedious labour, long lead times (Santos et al. 2017) and costly
78 orthoses.

79 Therefore, this paper presents a novel methodology of using an affordable Fused
80 Deposition Modeling (FDM) 3D printing technology to develop an ankle brace designed with
81 metamaterial structures that mimic the human ligament properties. An ankle inversion sprain
82 injury is caused by an improper inverted or supinated landing position (Fong et al. 2009; Wright
83 et al. 2000). The vertical ground reaction force will then act medially to the subtalar joint axis,
84 and this consequently results in a large inversion or supination moment (Fong et al. 2009;
85 Wright et al. 2000). Secondly, lateral peroneal muscles could not restrain the ankle inversion
86 in time, leading to an ankle sprain injury (Fong et al. 2009). Yet, the use of ankle braces was
87 also found to reduce muscle activity of the lower extremity during rehabilitation (Feger et al.
88 2014). Braces should therefore be designed to complement rather than replace muscle use,
89 thereby weakening them. Hence, this novel ankle brace design aims to allow a functional range
90 of motion during sports. Yet, the ankle brace is also designed to reduce ankle inversion velocity
91 to allow the peroneal muscles to react in time to reduce ankle sprain injury risks. Benchtop
92 testing was conducted to test the performance of the ankle brace prototype for proof-of-concept
93 purposes.

94

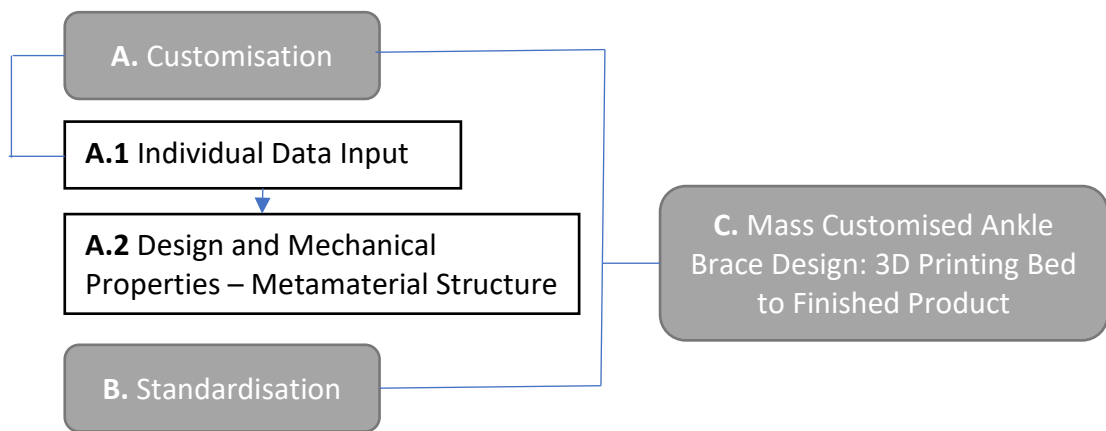
95 **2. Materials and Methods**

96 Design considerations of orthoses include production time, cost, weight, practical use,
97 durability, as well as attachment and removal (Santos et al. 2017). The ankle brace designed in
98 this paper aimed to be simple, easy to manufacture, affordable, lightweight, and functional for
99 sports play to reduce injury risks. It was not designed to replace the role of the muscles and
100 ligaments in the ankle joint but to reduce ankle inversion velocity for the muscles to react in
101 time to resist the ankle inversion loads. Thus, the brace was designed with little or no restriction

102 to high inversion moments to overcome the inadequacies of existing semi-rigid braces in the
103 market.

104 To allow the ankle brace to be fully customizable, a typical method would be to 3D
105 scan the foot before designing the ankle brace around the foot (Santos et al. 2017). However, a
106 fully customized ankle brace can be time consuming and expensive. Mass customisation could
107 be an alternative method of manufacturing to allow for personalisation at a more affordable
108 cost using standard mass-production methods (Hu 2013). This method is therefore adopted in
109 the manufacturing processes of the ankle brace prototypes, with the incorporation of the FDM
110 technology. Customization is only applied to the areas that require customized protection. The
111 other portions of the ankle brace will adopt a standard design workflow. Figure 1 shows the
112 workflow used in the development of the ankle brace in this paper.

113 <Figure 1 is inserted here>



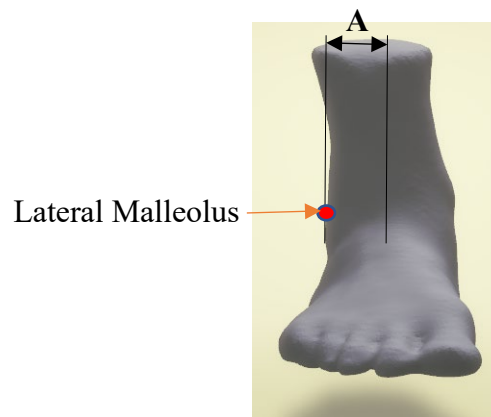
114
115 **Figure 1:** Design and Development Workflow for the Design of the Ankle Brace

116 117 **2.1 Individual Data Input Guided by Biomechanics**

118 To develop an ankle prototype for proof-of-concept in this paper, the anthropometry data of
119 the main author was collected as the subject for simplicity. The study was approved by the
120 Nanyang Technological University Institutional Review Board (IRB-2021-02-017). According

121 to Wei and others (2015), the ankle joint inversion moment during a Grade 1 ankle sprain was
122 23 Nm and the ankle external moment that caused pain and discomfort was 10 Nm. The
123 moment experienced during pain and discomfort at 10 Nm was chosen as a key parameter in
124 the design of this prototype. The distance A from the centre of the right ankle joint to the lateral
125 malleolus was 4.1 cm.

126 <Figure 2 is inserted here>



127

128 **Figure 2:** Distance A between the centre of the right ankle joint and the lateral malleolus.

129

130 Thus, the ankle brace was designed to resist the following force at 10 Nm external moment
131 minimally:

132
$$Force = \frac{Moment}{Distance A} = \frac{10}{4.1/100} = 244 N \quad (1)$$

133

134 Chu and others (2010) found that the maximum ankle inversion angles during common
135 sporting motion (running, cutting, jump landing, stepping down) was less than 10°. Thus, the
136 ankle brace should allow free movement within 10° of ankle inversion angle by having as
137 low a Young's modulus and inversion moment as possible at this range of motion. There
138 should then be an increase in Young's modulus and inversion moment beyond this point to
139 reduce inversion velocity for the brace to function. Based on the subject's measurements, the

140 ankle brace was designed to allow 10% of skin surface strain at 10° of ankle inversion angle
141 and 33% strain at maximum inversion range of motion at the lateral aspect of the brace. The
142 amount of skin surface strain was estimated using a measuring tape, with the foot at neutral,
143 at the ankle inversion angle of 10° and at maximum inversion range of motion using the
144 isokinetic dynamometer (Biodex System 4 Pro, Biodex Medical Systems, Inc., Shirley, NY,
145 USA). Young's modulus of the metamaterial structure specimens in the next section was
146 tested using the tensile test machine (Instron 5569, Instron Corporation, Norwood, MA,
147 USA) to ensure that the design was within the specifications.

148

149 ***2.2 Metamaterial Structure***

150 ***2.2.1 Prototype A – Diamond Mesh Design***

151 The mesh diamond metamaterial structures were first adopted, drawing inspiration from the
152 human ligament and mesh packaging. They were simple to implement yet provided different
153 Young's moduli at different stages of loading, simulating the viscoelastic properties of the
154 human ligament (Figure 3). The diamond mesh would stretch easily, flexing the diamond
155 structures (see Figure 3, Zone I) until the diamond structures became fully elongated and
156 straightened. After which, a higher force was required to stretch the diamond structures, as
157 illustrated in Figure 3 (Zone II). Threshold strain was set at 10% of strain at 10° of ankle
158 inversion angle based on the measurements made in the previous section.

159

160

<Figure 3 is inserted here>

161
162
163
164
165
166
167
168
169
170
171
172
173
174
175
176
177
178
179
180
181
182
183

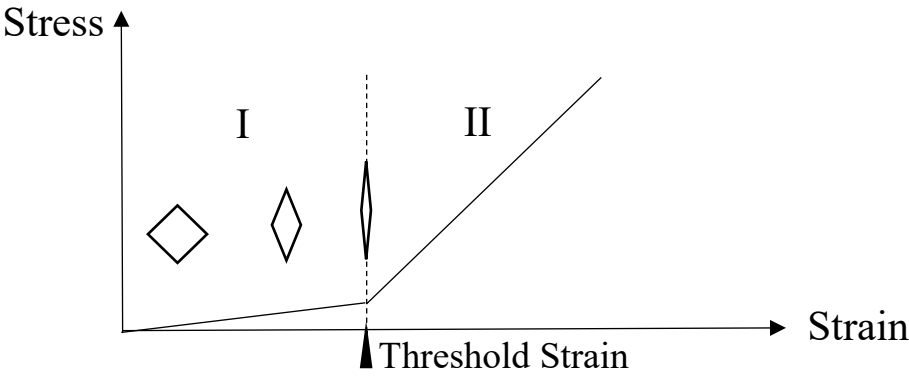


Figure 3: Stress-strain curve of the diamond metamaterial structures.

Traditionally, such mesh diamond metamaterial structures are manufactured using double extrusion. However, customization is difficult using the conventional double extrusion method compared to additive manufacturing or 3D printing. In addition, the diamond structures are asymmetrical, thus introducing anisotropic material properties. In one direction (direction A), applying the axial force allows the material to stretch easily (see Figure 4a). Conversely, applying the axial force in the transverse direction (direction B) allows the material to stretch less easily (see Figure 4b). Structures can thus be printed to create customized tensile properties in different regions and directions. These properties are influenced by parameters such as type of geometric shape, size of geometric shape (diameter of the printed polymer), and shape thickness.

<Figure 4 is inserted here>

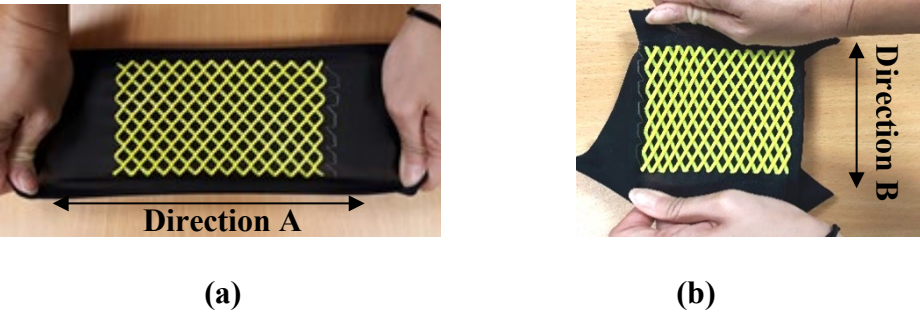


Figure 4: Material a) stretches easily in one direction b) but less easily in the transverse direction.

184 Figure 5 shows the tensile properties of the material in directions A and B. Young's modulus
185 could be adjusted by just varying the design parameters, such as the thickness and diamond
186 gap length (Figure 5). Direction A had a Young's modulus that was too low to be practical.
187 Direction B instead had a Young's modulus that was too high to allow a free functional range
188 of motion before threshold strain. To meet the design specifications such that a practical cross-
189 sectional area was provided to meet the targeted 244 N of loads, a hybrid design combining the
190 previous two designs in both directions (prototype A) was adopted. This will form the first
191 customized structure to restrain the ankle at positions beyond the functional range of motion.
192 This structure's dimensions are modified based on the individual data input for customization.
193 For this study, length of H was 20% of length of V (Figure 5). In the cross-sectional view of
194 the triangular sections, dimension T was 3 mm for direction B and 2.5 mm for direction A.
195 Dimension A was two thirds of dimension W (Figure 5).

196

197

<Figure 5 is inserted here>

198

199

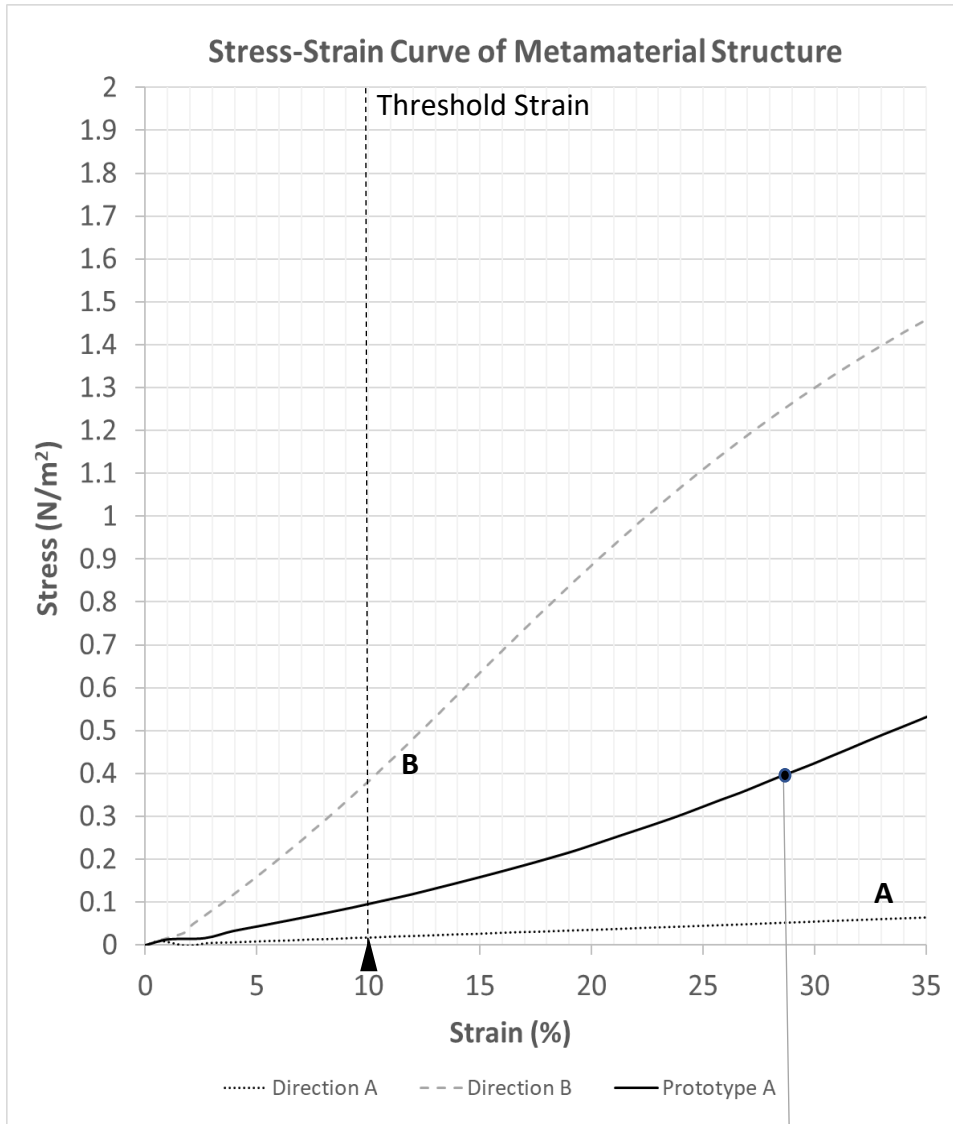
200

201

202

203

204



205

206

207

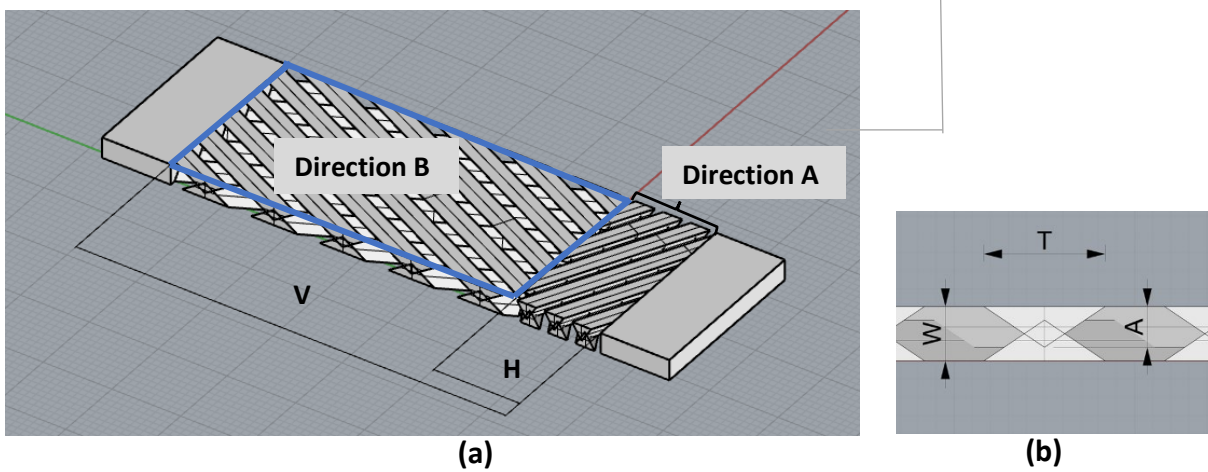
208

209

210

211

212



213

214

215

Figure 5: Stress-strain diagram of the diamond mesh structure in directions A and B and the hybrid design (prototype A). Young's modulus will increase after 'threshold strain' beyond the functional range of motion to restrain the ankle. Details of dimensions were that (a) length

216 of H was 20% of length of V and (b) in the cross-sectional view, dimension T was 3 mm for
217 direction B and 2.5 mm for direction A. Dimension A was two thirds of dimension W.

218
219 To achieve the properties as stated above, 3D printing had to be carried out. The top and bottom
220 layers of the structures were printed separately, such that pivoting was allowed during axial
221 load (Figure 6). Traditional 2D manufacturing techniques such as laser cutting will not allow
222 such pivoting structures to be obtained with a single cut. Besides, such 2D manufacturing
223 techniques will result in undercut issues in the 3D structures in this prototype A design.

<Figure 6 is inserted here>

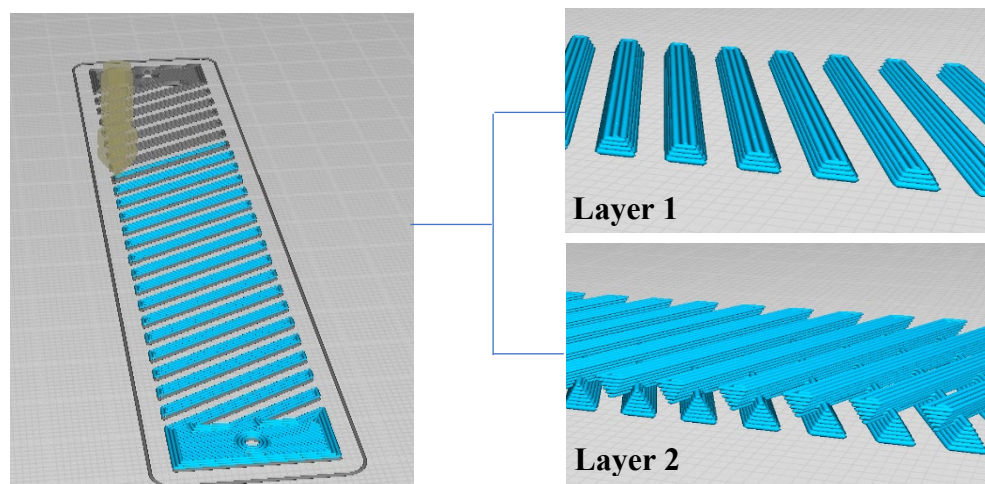


Figure 6: Printing of the metamaterial structure by two layers to allow for pivoting

2.2.2 Prototype B – Oriental Design

235 The “square grid” structure (Kolken and Zadpoor 2017) was found to provide a low Young’s
236 modulus in the functional range of motion. However, beyond the functional range of motion,
237 its Young’s modulus was too low to restrain the forces required in an ankle brace. The
238 “square grid” structure was thus modified to improve the Young’s modulus required for the
239 ankle brace specifications (Figure 7). During the design process, a series of iterations were
240 made with the support of simulation using SOLIDWORKS (Student Edition v2020, Dassault

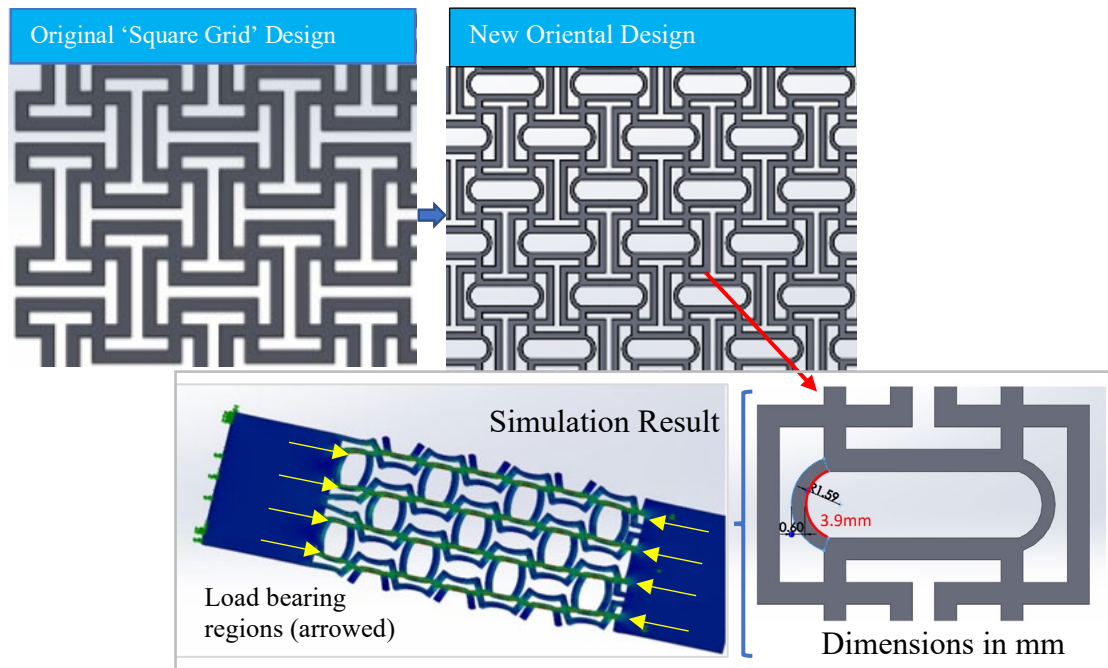
241 Systèmes SolidWorks Corporation, Waltham, MA, USA) to identify areas of load-bearing. In
242 the design, arches were included to allow for better flexing of the material within the
243 functional range of motion as the arches straighten up. Beyond the functional range of
244 motion, the applied load would stretch the arches and act as additional load-bearing structures
245 of the design. Arches were modified in terms of dimensions and positions of application to
246 limit Young's modulus within the functional range of motion and increase Young's modulus
247 beyond that. The 'I' structures were also modified to include larger sizes to allow space for
248 arches to be modified more effectively. The final design is shown in Figure 7.

249 The Young's modulus increased after the 'threshold strain', beyond the functional
250 range of motion. Unfortunately, Young's modulus also increased within the functional range
251 of motion before the threshold strain point with the additional arch support (Figure 8). This
252 would result in higher moments required for ankle inversion in the functional range of motion
253 during sport. However, Young's modulus in the functional range of motion is comparable to
254 Prototype A.

255

256

<Figure 7 is inserted here>



257

258

259

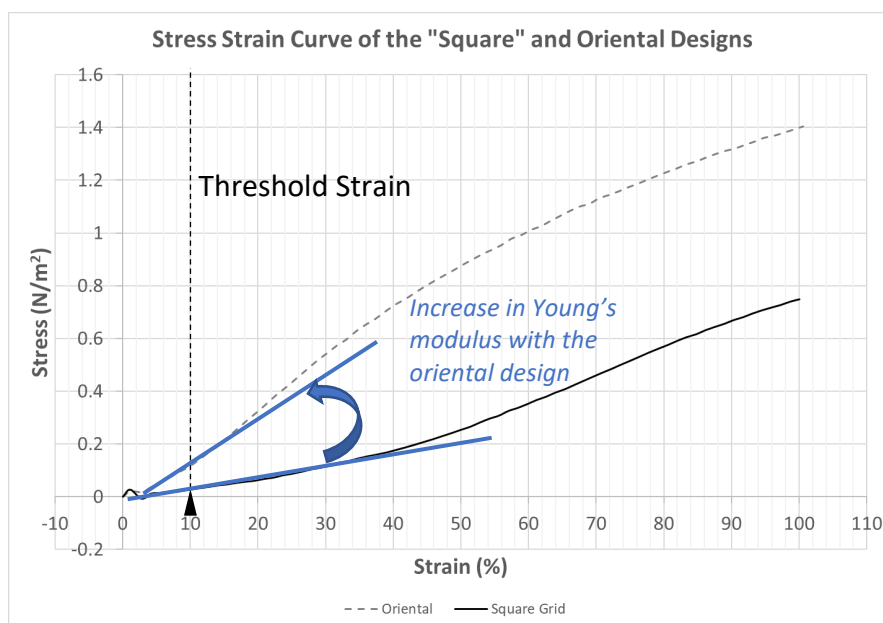
260

261

262

Figure 7: Oriental design modified from the “square grid” design (Kolken and Zadpoor, 2017) with dimensions in mm. As load applied, simulation results showed that the arch could provide additional support to the structure (along arrowed regions).

<Figure 8 is inserted here>



263

264

Figure 8: Stress-strain diagram of the “square grid” and oriental designs.

265 **2.2.3 Prototype C – “Horseshoe” Design**

266 The “horseshoe” structure was designed to imitate the stress-strain behavior of the human
267 skin (Jang et al. 2015). The base shape of the triangular lattice is an equilateral triangle.
268 Although the horseshoe structure can be adapted to other lattice configurations such as the
269 honeycomb, Ma and others (2016) determined that the triangular configuration allowed for
270 the sharpest transition at the critical strain required. The generalized stress-strain curve of the
271 “horseshoe” structure could be obtained by the normalized width ($\bar{w} = w/R$) and the arc angle
272 (θ), where w denotes the width of the curved beam used to make up the horseshoe structure
273 and R denotes the radius of the horseshoe structure curvature (Figure 9) (Ma et al. 2016).
274 Additionally, according to Zhang and others (2013), the width of individual beams of the
275 structure should be much thinner than the thickness of the structure to avoid out-of-plane
276 deformation. The equilateral triangle was designed using the dimensions $R = 10$ mm, $w = 0.5$
277 mm, arc angle = 90° for this proof-of-concept.

278

279 <Figure 9 is inserted here>

280

281

282

283

284

285

286

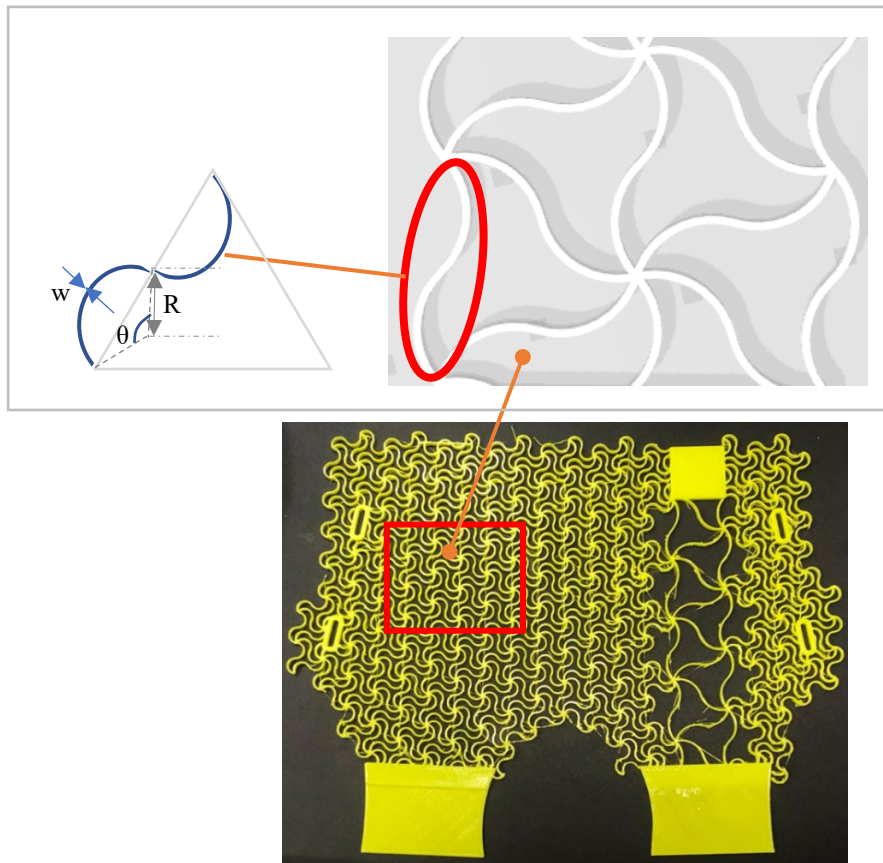
287

288

289

290

291



292

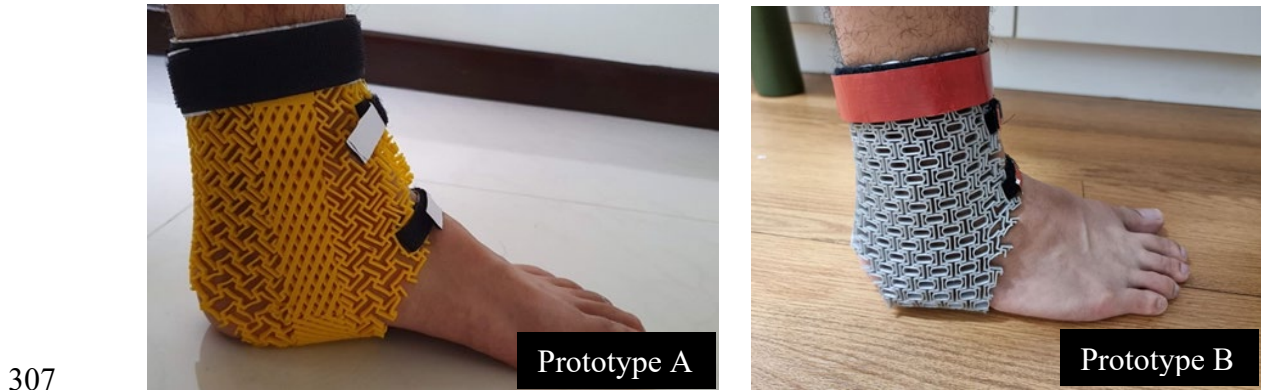
293 **Figure 9:** Parameters of the “horseshoe” structure: normalized width ($\bar{w} = w/R$) and the arc
294 angle (θ), where w denotes the width of the curved beam used to make up the horseshoe
295 structure and R denotes the radius of the horseshoe structure curvature (Ma et al. 2016).

296 **2.3 Non-functional Area of Brace**

297 For the rest of the ankle brace structure, the “square grid” structure (Kolken and Zadpoor,
298 2017) was used for metamaterial Prototypes A (diamond mesh design) and B (oriental
299 design), modifying the dimensions to fit the metamaterial structure used (Figure 10). This
300 structure was used in the prototype as preliminary results showed that it wrapped seamlessly
301 onto body joints, resulting in increased comfort. The last design, Prototype C (“horseshoe”
302 design), was designed entirely with the “horseshoe” structures (Figure 10). Flexible
303 thermoplastic polyurethane material (NinjaFlex, NinjaTek, Fenner Inc., Manheim, PA, USA)

304 with a shore hardness of 85A and tensile modulus of 12 MPa was eventually selected to allow
305 minimal resistance during the functional range of motion.

306 <Figure 10 is inserted here>



310 **Figure 10:** Ankle brace prototype A (diamond mesh design), prototype B (oriental design)
311 and prototype C (“horseshoe” design)

312

313 2.4 Design Features and Processes

314 *Design Considerations*

315 There have been many ankle braces in the market. The purpose of the ankle brace used in this
316 paper was not to out-perform these braces. Rather, the brace was to slow down the ankle
317 inversion velocity, allowing the peroneal muscles to restrain the ankle inversion in time.

318 **2.4.1 3D printing of a customised ankle brace**

319 For the ankle brace to be 3D printed, the brace needed to be laid out and printed on the flat
320 print bed. Drawing inspirations from socks and commercial braces, a “butterfly”- like design
321 was used as a standard design template for all individuals (Figure 11). The designs were
322 carried out using the design software (Rhino 6 Education Lab Version, Robert McNeel &
323 Associates, Seattle, WA, USA). The red regions are where customization was carried out
324 using the metamaterial structure described earlier.

325 <Figure 11 is inserted here>

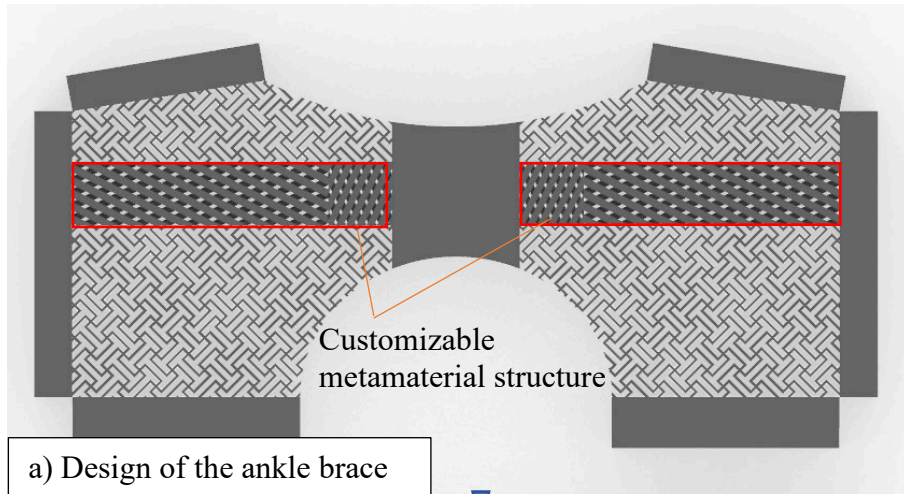
326

327

328

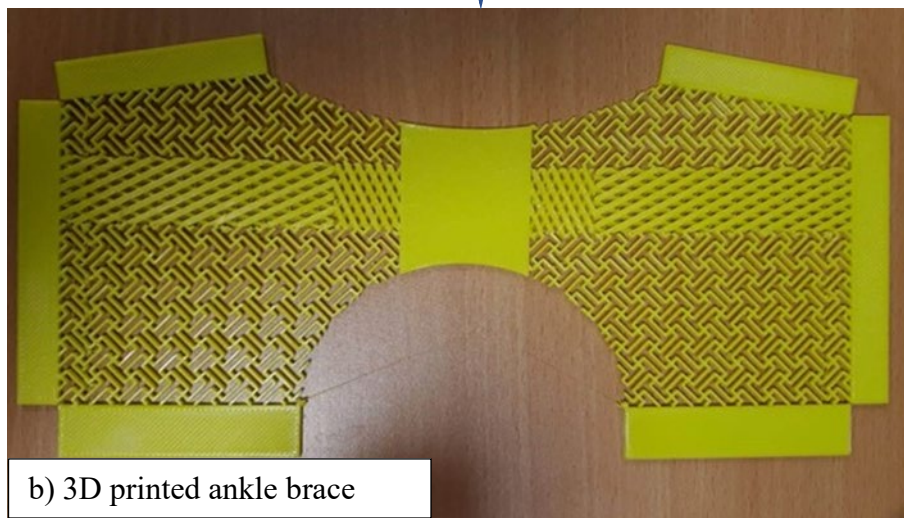
329

330



331

a) Design of the ankle brace



332

b) 3D printed ankle brace



333

c) 3D printed ankle brace on the foot

334 **Figure 11:** a) Design of the ‘butterfly’ ankle brace with red zones for customized protection;

335 b) 3D printed brace laid out flat on the print bed; and c) 3D printed ankle brace on the foot.

336

337 The ankle brace was then printed using a LulzBot FDM 3D Printer (TAZ 5, Fargo Additive

338 Manufacturing Equipment 3D, Fargo, ND, USA) fitted with a FlexyStruder extruder head.

339 ***Benchtop Testing for Proof-of-Concept***

340 Competitive analysis was conducted on the prototype ankle brace, with respect to other
341 commercially available braces:

- 342 • Prototype ankle brace
- 343 • Semi-Rigid: Donjoy PRO Ankle Brace
- 344 • Semi-Rigid, Hinge Design: Ultra Zoom Ankle Brace
- 345 • Lace-up Design: Med Spec ASO Ankle Stabilizer
- 346 • Sleeve Design: Saibike Ankle Support

347

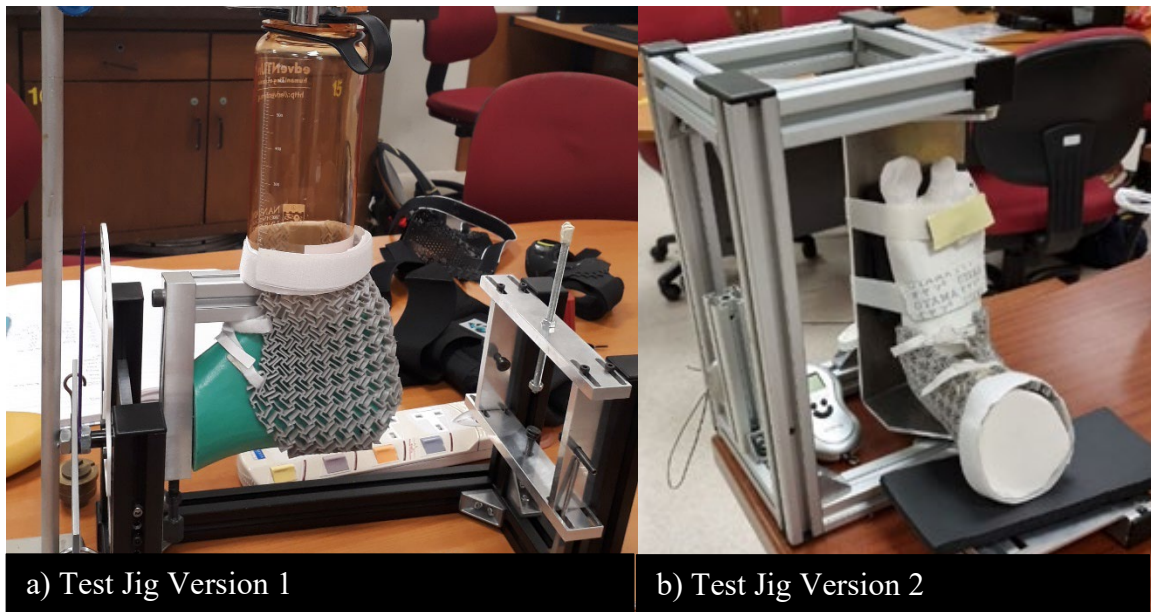
348 Range of motion benchtop testing was conducted on the main author using the isokinetic
349 dynamometer (Biodex System 4 Pro, Biodex Medical Systems, Inc., Shirley, NY, USA) and
350 using a goniometer (Lafayette Gollehon Extendable Goniometer, Lafayette Instrument,
351 Lafayette, IN, USA) to measure the maximum plantar flexion angles. For each ankle brace,
352 zero position was set at the ankle's neutral position when the foot was relaxed. The range of
353 motion test was also conducted in the barefoot condition.

354

355 A test jig version 1 was first built, followed by a test jig version 2, to measure the moment
356 required to invert the ankle to 10° and 30°. The jigs are seen in Figure 12. A 3D printed foot
357 with a ball and socket joint at the ankle was also manufactured for the test jig version 2. A
358 foot plate was designed and oriented such that the axis of rotation was vertical and parallel to
359 direction of the weight of all the parts, thus avoiding the need to incorporate weight into the
360 force calculations for version 2 (Appendices 1 - 3). Prototypes B and C were unavailable
361 when the test jig version 1 was used. Test jig version 2 also could not fit the lace-up design,
362 and test results from both jigs were thus included. A portable electronic scale (Weiheng
363 portable electronic scale, Guangzhou Weiheng Electronics, Guangdong, China) was used to

364 measure the force required to rotate the ankle brace. A ratio was calculated to indicate the
365 amount of moment required to invert the ankle to 30° over 10°. A bigger ratio shows that
366 increased moment is required to invert the ankle beyond the functional range of motion
367 compared to within.

368 <Figure 12 is inserted here>



370 **Figure 12:** Two test jig versions 1 and 2 were built to measure the moment required to invert
371 the ankle brace to 10° and 30°. A 3D printed foot with a ball and socket joint at the ankle was
372 also manufactured for test jig version 2.

373 **Results**

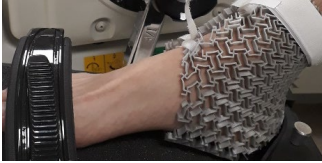



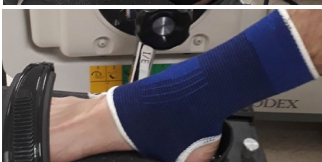
374 Table 1 shows the results of the range of motion of the prototype ankle braces
375 compared to four commercially available ankle brace products. The prototype ankle braces
376 allowed full plantar range of motion, similar to barefoot testing. The other commercial
377 braces, especially the semi-rigid hinge design, resulted in a reduced plantar range of motion
378 (Range: 1° to 12° reduction in plantar flexion angles).

379

380 < Table 1 is inserted here >

381

382 **Table 1:** Maximum ankle plantar flexion angles of the prototype ankle brace compared to other
 383 commercially available ankle braces.

Type of Ankle Brace	Images	Category of Ankle Brace	Maximum Ankle Plantarflexion Angle (°)
Barefoot	-	-	50
Prototypes A, B and C		3D Printed	50
Donjoy POD		Semi-Rigid	41
Ultra Zoom		Semi-Rigid, Hinge	38
Med Spec ASO Stabilizer		Lace-Up	43
Saibike Ankle Support		Sleeve	49

384

385

386 Table 2 shows the amount of moment required to invert the ankle to 10° and 30°. The prototype
 387 braces B and C had ratios comparable to the commercial Donjoy POD product, which was the
 388 best performing commercial product in this aspect. Prototype A was comparable to the sleeve
 389 product in terms of the ratio. Moments required to rotate the ankle at the functional range of
 390 motion (less than 10°) among the prototype braces were lower than all other commercial
 391 products except the sleeve design (Saibike Ankle Support).

392

393

< Table 2 goes here >

394 **Table 2:** Moment to invert prototype and commercially available ankle braces to 10° and
 395 30°. Prototypes B and C were unavailable when the test jig version 1 was used. Test jig
 396 version 2 also could not fit the lace-up design, and these results were excluded.

Type of Ankle Brace	Category of Ankle Brace	(A) Test Jig Version 1			(B) Test Jig Version 2		
		(A.1) Moment for 10° Inversion (Nm)	(A.2) Moment for 30° Inversion (Nm)	Ratio (A.2/A.1)	(B.1) Moment for 10° Inversion (Nm)	(B.2) Moment for 30° Inversion (Nm)	Ratio (B.2/B.1)
Prototype A - Diamond Mesh	3D Printed	0.50	0.84	1.7	0.37	0.55	1.5
Prototype B - Oriental	3D Printed				0.31	0.92	2.9
Prototype C - Horseshoe	3D Printed				0.16	0.45	2.9
Donjoy POD	Semi-Rigid	0.71	1.91	2.7	1.15	3.27	2.9
Ultra Zoom	Semi-Rigid, Hinge	1.76	3.37	1.9	0.98	1.85	1.9
Med Spec ASO Ankle Stabilizer	Lace-Up	1.90	3.57	1.9			
Saibike Ankle Support	Sleeve	0.44	0.59	1.3	0.15	0.22	1.5

397

398

399 Discussion

400 This paper aims to illustrate a new methodology of using an affordable FDM 3D
 401 printing technology to develop an ankle brace designed with metamaterial structures that mimic
 402 human ligament properties. Three prototypes were developed as a proof of concept,
 403 incorporating the metamaterial structure, customized to each individual.

404 The prototypes required one of the lowest moments during the functional range of
 405 motion and yet achieved almost twice or thrice the moment required beyond that range. All the
 406 commercial braces allowed a free functional range of motion of 10°. However, more effort or
 407 moment was required to rotate the ankle for most of these tested braces than for our prototype
 408 ankle braces. This suggests that the 3D printed prototype braces achieved their purpose of
 409 allowing low moments for easy ankle inversion in the functional range of motion.

410 Beyond the functional range of motion, the moments of the prototype braces increased
 411 by almost two to three times, with similar performances with the commercial ankle braces,
 412 especially for prototypes B and C. This could help slow motion down in this range. However,
 413 the actual moments of the prototypes (Range: 0.45 Nm – 0.92 Nm) were much less than
 414 commercial products (Range: 0.22 Nm – 3.27 Nm) using the self-designed jig Version 2 as the
 415 prototype ankle braces were not designed to be stiff enough to replace the player’s muscles.
 416 Overall, the Donjoy POD seemed to perform the best among the commercial braces with the

417 highest ratio in terms of the moment required at 30°, compared to at 10° of ankle inversion.
418 Prototype B and C had a comparable ratio (2.9) as the Donjoy Pod. Prototype B had a higher
419 moment required than prototype C for better protection at 30° of inversion. However, prototype
420 B also had a correspondingly higher moment required to invert the test jig ankle to 10° than
421 prototype C and this could affect the performance in the functional range of motion.
422 Nevertheless, prototype C could not resist the moments required to invert the test ankle to 30°
423 and went into plastic deformation soon after that. Collectively, prototype B would be a better
424 choice for the 3D printed ankle brace.

425 Initial tests also showed that as designed, the prototype ankle braces allowed full plantar
426 range of motion, similar to barefoot testing. This was unlike the other commercial braces,
427 especially the semi-rigid and lace-up designs, resulting in a reduced plantar range of motion.
428 Ankle plantar flexion is required to help in force absorption (Alentorn-Geli et al., 2009). On
429 average, ankle plantar flexion angles were less than 30° (Mean 29° SD(8°)) during natural
430 single-leg landings (Teng, Leong and Kong 2020). Therefore, while restrictions of plantar
431 flexion angles were observed, all the braces could still allow functional plantar flexion range
432 of motion in single-leg landings (Table 1). However, a more effective way of assessment was
433 to measure the moment required to reach the plantar range of motion. This was not measured
434 during the test as this was not the focus of the study, and the test jigs were not designed to
435 measure this. The semi-rigid hinge and lace-up braces probably required more effort to produce
436 similar ankle plantar flexion angles as the prototypes.

437 Together, the prototypes have achieved their design purposes for proof-of-concept.
438 FDM has allowed for mass customization with unique properties at selected regions based on
439 individual needs and at relatively affordable costs. Using 3D printers with higher resolution to
440 print more refined structures or sourcing for other flexible 3D printed materials could further
441 reduce the inversion moment in the functional range of motion. Comparatively, more

442 traditional 2D manufacturing methods such as laser cut could be simpler to use and faster to
443 manufacture. Yet, these 2D methods do not allow for more complex 3D structures to be
444 manufactured. Besides, such 2D methods may have 'undercut' issues for 3D structures such as
445 that found in prototype A. Also, for prototype A, the upper and lower layers must be printed
446 separately for the 'pivoting' effect to work to allow greater flexibility in the functional range of
447 motion. This could not be achieved using laser cutting when the structures are cut out in one
448 sequence. Furthermore, although this paper used 2D structures as a proof-of-concept in
449 prototypes B and C, 3D complex layers of different structures could be developed in future to
450 create more unique metamaterial properties in braces. Therefore, this paper aims to introduce
451 the methodology to design mass customized braces using 3D printing as the core technique.

452

453 *Conclusion*

454 This paper illustrates a new methodology of using an affordable FDM 3D printing technology
455 to develop an ankle brace designed with metamaterial structures that mimic human ligament
456 properties. A prototype was developed as a proof of concept, incorporating the metamaterial
457 structure, customized to each individual. Initial tests show that as designed, the prototype
458 braces maintained the full range of motion for plantar flexion angles. Initial tests also show
459 that the prototype requires one of the lowest moments during a functional range of motion,
460 yet achieving almost twice to thrice the moment required beyond the functional range of
461 motion. Unlike commercial ankle brace designs, the prototype designs could better allow
462 players to play without restrictions in the functional range of motion during sport. Yet, at
463 high-risk positions, the prototype designs could aid in reducing ankle inversion velocity to
464 allow the peroneal muscles to react in time to help in reducing ankle sprain injury risks.

465

466 **Text Word Count = 4319**

467 **Acknowledgements:** The authors would like to thank Chan Jinhao for his preliminary test
468 results using the “square grid” structures.

469

470 **Declaration of Interest Statement:**

471 The authors declare that there is no conflict of interest.

472

473 **Biographical note.**

474 Dr Phillis Teng is a senior research fellow at the Nanyang Technological University,
475 Singapore (NTU), with the passion in biomechanics research, especially in injury risk
476 reduction. She has a diverse background in biomechanics research and mechanical
477 engineering, with 6.5 years of industry experience as an Engineer at Hewlett-Packard
478 Singapore. She obtained her PhD in NTU in 2015 and her PhD research on ‘Investigation of
479 Foot Landing Techniques and Muscle Activation during Single-Leg Drop Landings:
480 Implications for Non-Contact Anterior Cruciate Ligament Injuries’ has produced 4 journal
481 and 4 conference papers. Her past 10 years in research included areas in sport injury risk
482 reduction; human perception in comfort and fit; mechanical shoe testing; 3D printed brace
483 development using metamaterial structures; and biomechanics study of customized 3D
484 printed insoles. She is now with the Rehabilitation Research Institute of Singapore, studying
485 knee osteoarthritis risks and exploring the possibility for an early biomechanics intervention.

486

487 A/P Kah Fai Leong is an associate professor in the School of Mechanical and Aerospace
488 Engineering, Nanyang Technological University. He obtained his B.Eng. (Mech.) with
489 Honours from the National University of Singapore in 1981 and M.Sc. degrees in
490 Engineering Product Design and Mechanical Engineering, from Stanford University in 1987.
491 Prior to joining NTU, he has worked several years as a product development engineer and

492 designer in the Singapore electronics industries. He was awarded the Merit Award in 1994
493 and Distinguished Award in 1997 for his contributions to the national standardisation
494 program. His research interests are in Additive Manufacturing for biomedical applications,
495 particularly in tissue engineering; sports technology; sports science; polymer matrix
496 composites; design science; and design education. He has co-authored five books, published
497 more than ten book chapters and more than 200 papers in international journals, conferences,
498 and seminars in these areas. He has been invited as a keynote speaker for a number of
499 premier conferences and has acted as reviewers for several journals, including Materials and
500 Design, Virtual and Physical Prototyping; Additive Manufacturing; Materials Today, Trends
501 in Biotechnology, Biomaterials, Acta Biomaterials, Journal of the Mechanical Behavior of
502 Biomedical Materials, amongst others.

503

504 A/P Pui Wah (Veni) Kong is the Associate Dean for Research Grants Management and an
505 Associate Professor at the National Institute of Education, Nanyang Technological
506 University, Singapore. Her research interests are sports and clinical biomechanics, with
507 applications in human performance, injury prevention and rehabilitation. Dr Kong has led
508 research projects on high-performance sports, gait, footwear, foot health, low back pain,
509 massage, and sports injuries. She conducted laboratory experiments and field tests on
510 athletes, school children, older adults, firefighters, paramedics, military personnel, and
511 patients with various musculoskeletal health conditions. She worked closely with hospitals,
512 clinics, government agencies and industrial partners to conduct interdisciplinary research that
513 can impact the society. She was the recipient of the Fellow of International Society of
514 Biomechanics in Sports (FISBS) in 2020, among other presentation awards from the
515 International Sports Engineering Association, British Association of Sport and Exercise
516 Sciences, Asian Society of Sport Biomechanics and Sports Medicine Association Singapore.

517

518 Mr Er Bin Hao created the template for ankle brace development as part of his final year
519 engineering project and is currently a UX designer, working on designing digital products
520 that help to solve the sustainability challenge. Having graduated from Nanyang
521 Technological University, Singapore with a Bachelor in Mechanical Engineering, he has
522 since pivoted to a career in user experience and design, working with companies to deliver
523 visual solutions and data driven metrics in order to help in energy management and carbon
524 net zero.

525

526 Mr Chew Zhi Yuan graduated from Nanyang Technological University in 2021 and obtained
527 a degree in Mechanical Engineering. For his final year engineering project, he re-designed
528 the existing metamaterial structure to improve its tensile properties and used simulation in his
529 design iterations. He also explored the use of printing on cloth to enhance the ankle brace
530 comfort levels.

531

532 Ms Tan Phei Shien graduated from Nanyang Technological University in 2021 and obtained
533 a degree in Mechanical Engineering with a specialisation in Design. She has worked on
534 various design projects throughout her undergraduate course and her work on utilizing
535 metamaterials in an ankle brace was her first research related project. She also designed and
536 developed the newer test jig to allow for ankle brace testing and competitive analysis.

537

538 Mr Chor Hiong Tee (Frankie) is a Project Officer at the Rehabilitation Research Institute of
539 Singapore, Nanyang Technology University, Singapore. His research interests include product
540 aesthetics, human-centered design and design strategies. Frankie has more than a decade of
541 design and research experience in the multimedia, advertising and industrial design industries.

542 Since graduating with a Bachelor of Fine Art in Product Design from Nanyang Technological
543 University (NTU), he has managed numerous research projects in academia and industrial
544 collaborations with commercial partners. As an industrial designer/design researcher, Frankie
545 is instrumental in developing various consumer products, ranging from home service robots
546 for the elderly, intelligent wearables for lifestyle needs, gears and equipment for sports and
547 medical rehabilitation applications. His collaboration with the Badminton World Federation
548 (BWF) to develop an outdoor shuttlecock solution has led to a successful commercial launch
549 of a new outdoor game called Air Badminton. In addition, Frankie has written a book chapter
550 and helped edit manuscripts for a collaborative book project on Digital Manufacturing for the
551 HP-NTU Corporate Laboratory in NTU.

552

553 **References**

- 554 1. Alentorn-Geli, E., G. D. Myer, H. J. Silvers, G. Samitier, D. Romero, C. Lázaro-Haro,
555 and R. Cugat. 2009. Prevention of non-contact anterior cruciate ligament injuries in
556 soccer players. Part 1: Mechanisms of injury and underlying risk factors. *Knee surgery,*
557 *sports traumatology, arthroscopy: official journal of the ESSKA* 17(7): 705–729.
558 <https://doi.org/10.1007/s00167-009-0813-1>
- 559 2. Bot, S.D.M., and W. van Mechelen. 1999. The effect of ankle bracing on athletic
560 performance. *Sports Medicine* 27(3): 171-178. [https://doi.org/10.2165/00007256-](https://doi.org/10.2165/00007256-199927030-00003)
561 [199927030-00003](https://doi.org/10.2165/00007256-199927030-00003)
- 562 3. Cha, Y. H., K. H. Lee, H. J. Ryu, I. W. Joo, A. Seo, D. H. Kim, and S. J. Kim. 2017.
563 Ankle-Foot Orthosis Made by 3D Printing Technique and Automated Design Software.
564 *Applied bionics and biomechanics* 2017: 9610468. <https://doi.org/10.1155/2017/9610468>
- 565 4. Chen, E. T., J. Borg-Stein, and K. C. McInnis. 2019. Ankle Sprains: Evaluation,
566 Rehabilitation, and Prevention. *Current sports medicine reports* 18(6): 217–223.
567 <https://doi.org/10.1249/JSR.0000000000000603>
- 568 5. Chu, V.W.-S., D.T-P. Fong, Y-Y. Chan, P.S-H. Yung, K-Y. Fung, and K-M. Chan. 2010.
569 Differentiation of ankle sprain motion and common sporting motion by ankle inversion
570 velocity. *Journal of biomechanics* 43(10): 2035 - 2038.
571 <https://doi.org/10.1016/j.jbiomech.2010.03.029>
- 572 6. Cordova, M.L., C.D. Ingersoll, and M.J. LeBlanc. 2000. Influence of ankle support on
573 joint range of motion before and after exercise: a meta-analysis. *Journal of Orthopaedic*
574 *& Sports Physical Therapy* 30(4): 170-182. <https://doi.org/10.2519/jospt.2000.30.4.170>
- 575 7. Feger, M.A., L. Donovan, J.M. Hart, and J. Hertel. 2014. Effect of ankle braces on lower
576 extremity muscle activation during functional exercises in participants with chronic ankle
577 instability. *International Journal of Sports Physical Therapy* 9(4): 476-487.

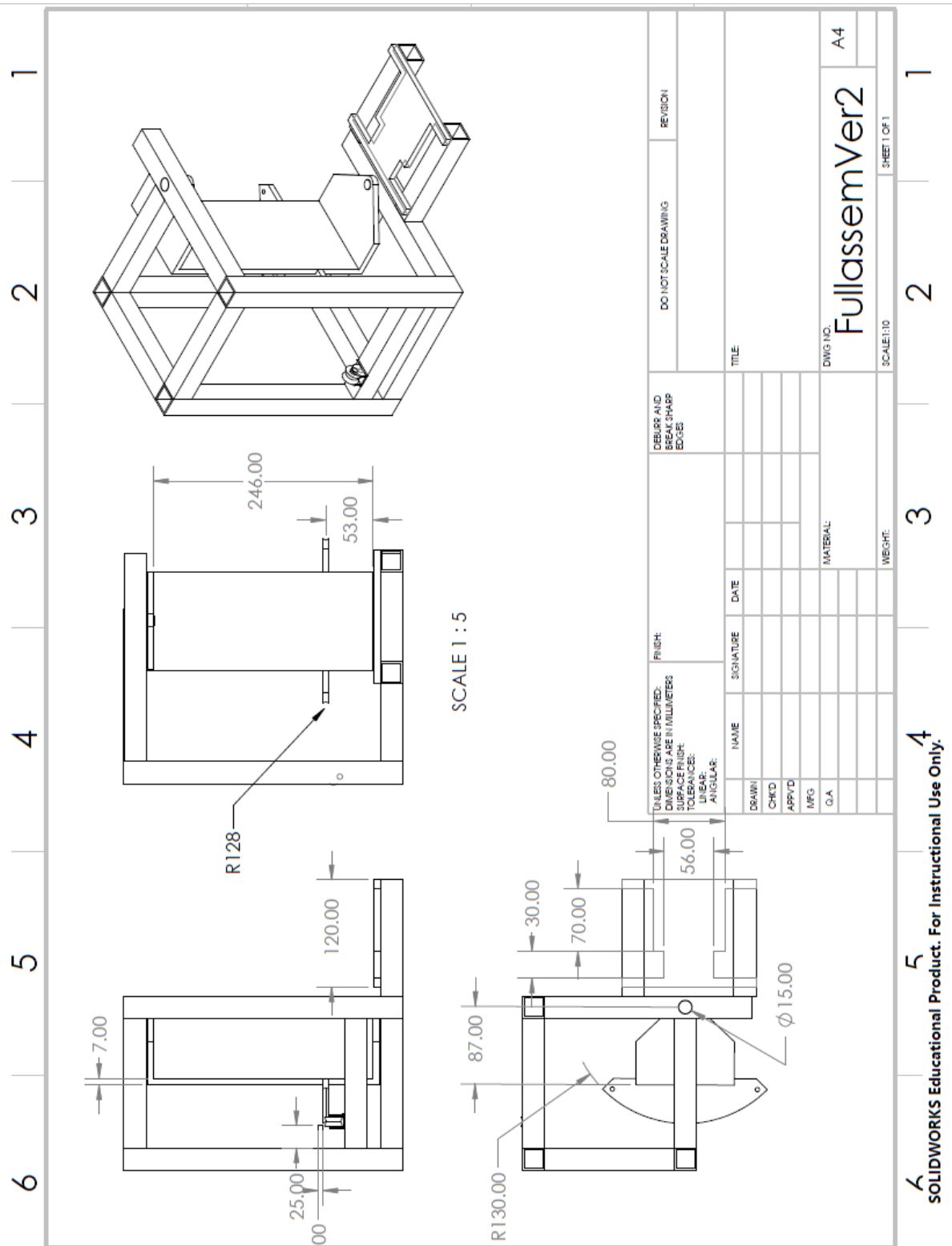
- 578 8. Fong, D.T.P., Y.Y. Chan, K.M. Mok, P.S.H. Yung, and K.M. Chan. 2009. Understanding
579 acute ankle ligamentous sprain injury in sports. *Sports Medicine, Arthroscopy,*
580 *Rehabilitation, Therapy and Technology*, 1: 14. <https://doi.org/10.1186/1758-2555-1-14>
- 581 9. Hu, S.J. 2013. Evolving Paradigms of Manufacturing: From Mass Production to Mass
582 Customization and Personalization. *Procedia CIRP* 7: 3–8.
583 <https://doi.org/10.1016/j.procir.2013.05.002>
- 584 10. Jang, K-I., H. U. Chung, S. Xu, C.H. Lee, H. Luan, J. Jeong, H. Cheng, G-T. Kim, S.Y
585 Han, J.W. Lee, and et al. 2015. Soft network composite materials with deterministic and
586 bio-inspired designs. *Nature Communications* 6: 6566.
587 <https://doi.org/10.1038/ncomms7566>
- 588 11. Kaminski, T. W., A. R. Needle, and E. Delahunt. 2019. Prevention of Lateral Ankle
589 Sprains. *Journal of athletic training* 54(6): 650–661. <https://doi.org/10.4085/1062-6050->
590 487-17
- 591 12. Kolken, H.M.A, and A.A Zadpoor. 2017. Auxetic mechanical metamaterials. *RSC*
592 *advances* 7(9): 5111-5129. <https://doi.org/10.1039/C6RA27333E>
- 593 13. Ma, Q., H.Y. Cheng, K.I. Jang, H.W. Luan, K.C. Hwang, J.A. Rogers, Y.G. Huang and
594 Y.H. Zhang. 2016. A nonlinear mechanics model of bio-inspired hierarchical lattice
595 materials consisting of horseshoe microstructures. *Journal of the Mechanics and Physics*
596 *of Solids* 90: 179-202. <https://doi.org/10.1016/j.jmps.2016.02.012>
- 597 14. Mann, B., A. H. Gruber, S. P. Murphy, & C. L. Docherty. 2019. The Influence of Ankle
598 Braces on Functional Performance Tests and Ankle Joint Range of Motion. *Journal of*
599 *sport rehabilitation* 28(8): 817–823. <https://doi.org/10.1123/jsr.2018-0315>
- 600 15. Parsley, A., L. Chinn, S.Y. Lee, C. Ingersoll, and J. Hertel. 2013. Effect of 3 different
601 ankle braces on functional performance and ankle range of motion. *Athletic Training &*
602 *Sports Health Care* 5(2): 69-75. <https://doi.org/10.3928/19425864-20130213-02>

- 603 16. Paulose, J., A. S. Meeussen, and V. Vitelli. 2015. Selective buckling via states of self-
604 stress in topological metamaterials. *Proceedings of the National Academy of Sciences -*
605 *PNAS* 112(25): 7639–7644. <https://doi.org/10.1073/pnas.1502939112>
- 606 17. Rowley, K.M., and J.G. Richards. 2015. Increasing plantarflexion angle during landing
607 reduces vertical ground reaction forces, loading rates and the hip’s contribution to support
608 moment within participants. *Journal of Sports Sciences* 33(18): 1922-1931.
609 <https://doi.org/10.1080/02640414.2015.1018928>
- 610 18. Santos, S., B. Soares, M. Leite, and J. Jacinto. 2017. Design and development of a
611 customised knee positioning orthosis using low cost 3D printers. *Virtual and Physical*
612 *Prototyping* 12(4): 322-332. <https://doi.org/10.1080/17452759.2017.1350552>
- 613 19. Telfer, S., J. Pallari, J. Munguia, K. Dalgarno, M. McGeough, and J. Woodburn. 2012.
614 Embracing additive manufacture: implications for foot and ankle orthosis design. *BMC*
615 *Musculoskeletal Disorders* 13: 84. <https://doi.org/10.1186/1471-2474-13-84>
- 616 20. Teng, P., K. F. Leong, and P. W. Kong. 2020. Influence of Foot-Landing Positions at
617 Initial Contact on Knee Flexion Angles for Single-Leg Drop Landings. *Research*
618 *quarterly for exercise and sport*, 91(2), 316–325.
619 <https://doi.org/10.1080/02701367.2019.1669765>
- 620 21. Wei, F., D.T. Fong, K.M. Chan, and R.C. Haut. 2015. Estimation of ligament strains and
621 joint moments in the ankle during a supination sprain injury. *Computer Methods in*
622 *Biomechanics and Biomedical Engineering* 18(3): 243-248.
623 <https://doi.org/10.1080/10255842.2013.792809>
- 624 22. Wright, I. C., R. R. Neptune, A. J. van den Bogert, and B. M. Nigg, 2000. The influence
625 of foot positioning on ankle sprains. *Journal of biomechanics* 33(5): 513–519.
626 [https://doi.org/10.1016/s0021-9290\(99\)00218-3](https://doi.org/10.1016/s0021-9290(99)00218-3)

627 23. Zadpoor, A.A. 2016. Mechanical meta-materials. *Materials Horizons* 3(5): 371-381.
628 <https://doi.org/10.1039/C6MH00065G>
629 24. Zhang, Y., S. Xu, H. Fu, J. Lee, J. Sun, K-C. Hwang, J.A. Rogers and Y. Huang, 2013.
630 Buckling in serpentine microstructures and applications in elastomer-supported ultra-
631 stretchable electronics with high areal coverage. *Soft Matter* 9(33): 8062-8070.
632 <https://doi.org/10.1039/C3SM51360B>

633
634
635
636
637
638
639
640
641
642
643
644
645
646
647
648
649
650
651
652
653
654
655
656
657
658
659
660
661
662
663
664
665
666
667
668
669
670

671 Appendix 1 – Engineering Drawing of full jig

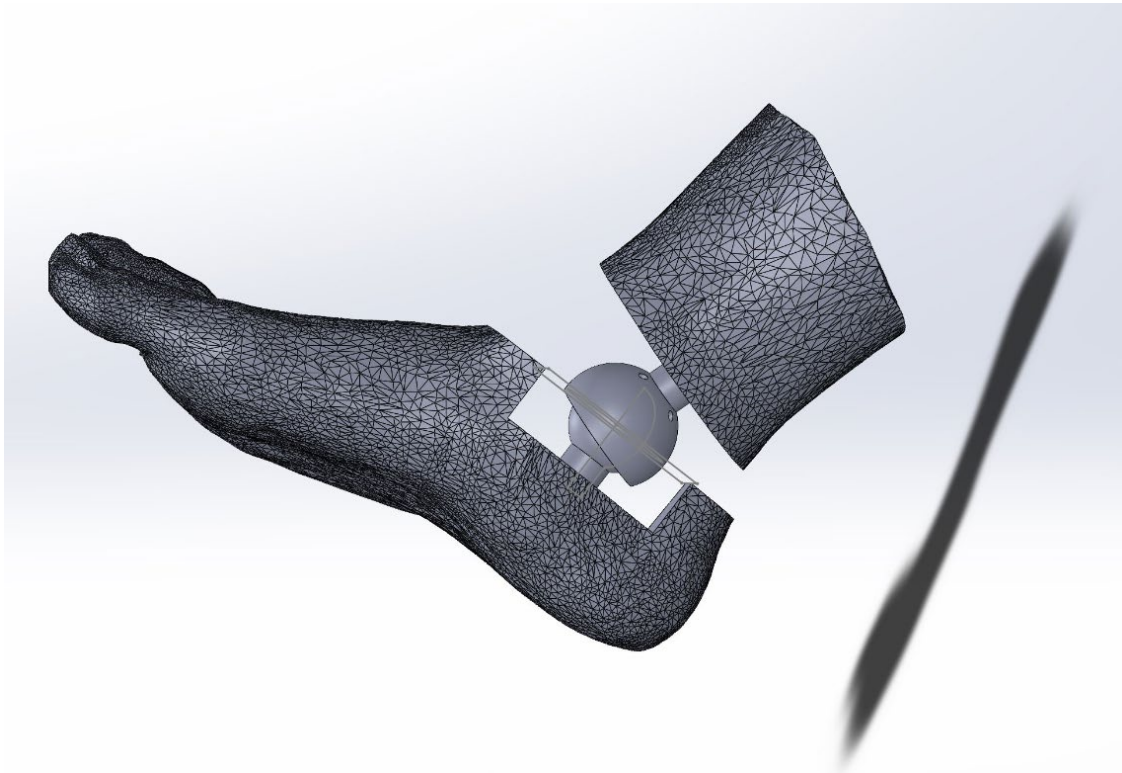


672

673

674

679 **Appendix 3 – CAD model of Foot with joint**



680